Investigation of Optimal Parameters for Oxide-Assisted Growth of Vertically Aligned Single-Walled Carbon Nanotubes

Cary L. Pint,[†,⊥,■] Sean T. Pheasant,[‡,⊥,■] A. Nicholas G. Parra-Vasquez,[§,⊥] Charles Horton,[⊥] Yaqiong Xu,[¶] and Robert H. Hauge*[,†,⊥]

Department of Physics and Astronomy, Department of Chemistry, Department of Chemical and Biomolecular Engineering, Richard E. Smalley Institute for Nanoscale Science and Technology, Rice University, Houston, Texas 77005, Department of Physics, Cornell University, Ithaca, New York

Received: August 7, 2008; Revised Manuscript Received: December 9, 2008

An investigation into the optimal growth of single-walled carbon nanotubes (SWNTs) in vertical arrays, or carpets, is presented utilizing atomic hydrogen catalyst activation with hot filament chemical vapor deposition. Using acetylene decomposition over Fe catalyst, we study the effect of oxidant-assisted growth using O_2, CO_2, and H_2O. Whereas trace amounts of O_2 result in the lack of any catalytic activity, CO_2 and H_2O are found to dramatically enhance the catalyst lifetime. On the basis of the saturation effect of oxidant concentration for both CO_2 and H_2O, we present this as being due to catalyst stabilization from surface hydroxyl groups, with H_2O having the most dominant effect upon carpet growth. Utilizing water-assisted growth, this process is further optimized to yield high-quality single-walled carbon nanotubes. High temperature growth (~775 °C) yields the highest-quality SWNTs, whereas controllable growth of double- and few-walled nanotubes can also be achieved at lower temperatures (550−600 °C). Finally, ultralong carpets are demonstrated by utilizing the optimal SWNT growth conditions under an enhanced carbon flux environment.

Introduction

Single-walled carbon nanotubes (SWNT)[1] are undoubtedly one of the most promising nanomaterials for the growing number of applications in the field of nanoscience and nanotechnology. With extraordinary mechanical, electrical, and thermal properties, research focusing on these nanoscale carbonaceous molecules is currently progressing at a remarkable rate. Although many applications have been already conceived for nanotubes since their discovery, the more recent observation that SWNTs can be grown from solid surfaces in aligned arrays[2] has introduced an ideal framework for materials which can be easily integrated into new and important applications. Some of the applications highly applicable to this growing field include field emission devices,[3] supercapacitors,[4,5] chemical sensors,[6,7] self-cleaning adhesive tapes,[8,9] and filtration membranes.[10,11] However, one of the fundamental limitations toward profound technological advances in these applications is the ability to have intricate control of the growth process. Control of nanotube diameter, number of walls, defect population, and other properties, such as length and SWNT density, will result in dramatic advances in each of these applications and increased potential for further applications.

On the basis of this concept, there has been a substantial effort to optimize the technique of growing aligned arrays of nanotubes. Recent efforts have been focused on the optimization of carpet growth with respect to SWNT yield based on novel synthesis methods.[12] However, this effort is concomitant to work by Hata et al.,[13,14] introducing the notion that H_2O-assisted growth with ethylene can be optimized to result in what is called "super-growth," or the rapid growth of SWNT material at rates of up to 2.5 mm in 10 min. In this study, Hata et al. observe that H_2O is an essential ingredient to extending the lifetime of the catalyst, etching defects and amorphous carbon to result in high-quality SWNT material. Following this work, there have been other studies which have utilized or considered H_2O as a component in nanotube array growth.[15−18] Although it is evident that the role of water is not yet fully understood, it is evident that the presence of a small, specific amount of water leads to growth enhancement, either in growth height or nucleation density. In addition, molecular oxygen has been observed to be a beneficial ingredient in some cases during growth of SWNT and MWNTs.[19−21] In the case of O_2-assisted methane decomposition,[20] a small amount of O_2 is found to reduce amorphous carbon and yield smaller-diameter distributions of nanotubes.

Recent observations by Kauppinen's group[22,23] have emphasized that both CO_2 and H_2O play an essential role in aerosol growth of SWNTs with a CO precursor. Analogous to super-growth conditions for gas-phase growth, CO_2 and H_2O additions to the reaction result in longer SWNTs, emphasizing the enhanced catalyst lifetime reported in other techniques. In this case, the role of the CO_2 and the H_2O is introduced as being an etching agent−synergistic with previous ideas on the role of these oxides during growth.

In addition to growth optimization in the presence of an oxidant, there have been more studies of the role of reactor parameters on the properties of nanotubes grown in aligned SWNT arrays.[24−26] Recent studies performed at Oak Ridge have demonstrated the use of a semiempirical growth modeling process to study aligned SWNT growth and its dependence on parameters such as temperature and carbon flux.[27,28] From this work emanates a simple, yet powerful concept that growth can be envisioned as a competition between the flux of incoming

* Author for correspondence. E-mail: hauge@rice.edu.
† Department of Physics and Astronomy, Rice University.
‡ Department of Chemistry, Rice University.
§ Department of Chemical and Biomolecular Engineering, Rice University.
⊥ Richard E. Smalley Institute for Nanoscale Science and Technology, Rice University.
¶ Department of Physics, Cornell University.
■ These authors are equal contributors to this manuscript.

10.1021/jp8070585 CCC: $40.75
Published on Web 02/16/2009

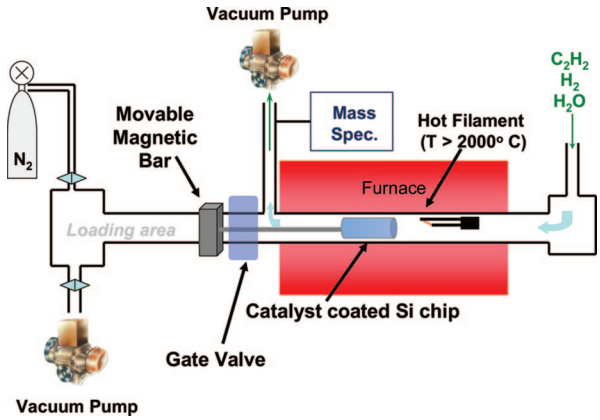

Figure 1. Schematic of carpet reactor utilized in this work.

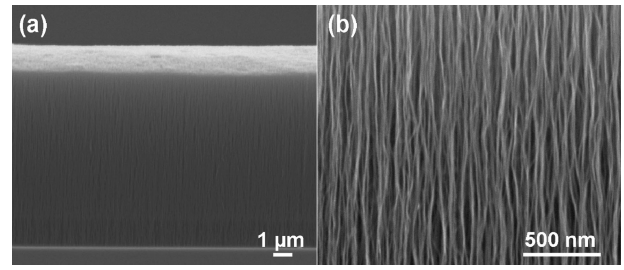

Figure 2. Characteristic scanning electron microscopy images of carpets grown by hot filament chemical vapor deposition. (a) Side-view image of a carpet showing the bundle structure, and (b) close-up view of the bundles showing the alignment of nanotubes in the carpet.

carbon and the rate at which carbon is deposited onto the growing nanotube. In this way, high-quality SWNT growth can be achieved at temperatures just before "poisoning", or the collective termination of SWNT growth, takes place. This means that the utilization of temperature and carbon flux as adjustable parameters in a CVD reactor can allow one to systematically adjust growth to a material with specific desired properties, such as quality and length. Such control in the optimization of the growth process suggests that higher yields of better-quality material can be easily achieved.

It is therefore the purpose of this study to first investigate the role of an oxidant during growth of aligned SWNTs utilizing CO_2-, H_2O-, and O_2-assisted growth. This allows us to determine a mechanistic understanding of the role of an oxidant during growth of carpets. In addition, we investigate the role of two parameters, temperature and carbon flux, on the properties of nanotubes grown in order to isolate the optimal conditions for high-yield, high-quality SWNT growth. With our results in qualitative agreement with previous modeling efforts, we present a universal picture of a highly adjustable, efficient growth technique that can be utilized for the synthesis of high-quality SWNTs, as well as other desired nanotube material.

Experimental Details

The hot filament chemical vapor deposition (HF-CVD) apparatus[29,30] utilized for the growth of vertically aligned carbon nanotube arrays (carpets) is illustrated in Figure 1. The reactor consists of a 1 in. tube furnace in which a 0.25 mm tungsten filament is suspended inside of a quartz tube near the center of the surrounding heating element. Control of the precursor gases is achieved by a gas manifold consisting of MKS mass flow controllers operated by LabView software. In a previous optimization scheme where we determined the optimal gas flow rates for aligned nanotube growth without the presence of an oxidant,[31] we found that growth was achieved with 400 standard cubic centimeters (sccm) of H_2 and 2 sccm C_2H_2. Under these precursor gas flow rates, the gas pressure monitored directly downstream of the furnace via a capacitance monometer is found to be stabilized at ~1.5 Torr (~ 200 Pa), with a flow rate of ~ 5 m/s. As illustrated in Figure 1, downstream of the furnace is a gate valve lode lock which isolates the sample loading area from the gas flow. This allows for the rapid interchange of samples without any disruption to the gas flow or exposure to air between subsequent experiments. Before, during, and after growth, the reaction gas mixture is sampled by both a Fourier transform infrared spectrometer, and a Dycor residual gas analyzer mass spectrometer (downstream from the reaction). While not in use, the whole system is kept under high vacuum with a turbomolecular pump (~$1-5 \times 10^{-6}$ Torr, $1.3-6.6 \times 10^{-4}$ Pa), and all incoming gas lines are resistively heated to evacuate all residual moisture. Combined, these measures allow us intricate control of the growth process with respect to the gases flowing and any contaminants which may be present in the reactor.

In order to grow carpets, the following steps are taken, (i) the furnace temperature is set and achieved, (ii) the hot filament is turned on by ramping to a current of ~10 A through the tungsten filament (while gases are flowing), and (iii) the gate valve is opened and the sample holder is moved to a point that is approximately 2 mm from the filament. The role of the hot filament is to achieve rapid reduction of the catalyst from a stable Fe_2O_3 to metallic (and catalytically active) Fe. This occurs due to the formation of atomic hydrogen while the filament is activated, as the high temperature of the filament (typically ~2500 °C) can dissociate H_2. The use of the hot filament is well-known in CVD diamond growth, where atomic hydrogen production has been experimentally characterized.[32] After 30 s of atomic hydrogen exposure from the hot filament, it is turned off, and growth takes place typically for an additional 30 min. The scheme in Figure 1 shows the reactor in the state that it typically remains during growth. After growth, the sample is moved outside the gate valve into the loading chamber, sealed, and purged with N_2 to allow efficient sample interchange. Following the insertion of a new sample, the loading chamber is evacuated and the sample holder is again moved inside of the reactor.

Water vapor is introduced in the system by bubbling H_2 through nanopure water at ~207 kPa (30 psig) upstream from an MKS 200 sccm mass flow controller. In order to degas the water, it is frozen with an acetone−dry ice bath and allowed to thaw under vacuum. This is cycled three times before the water vapor is brought into the reactor.

The typical growth substrate consists of 0.5 nm of Fe that is deposited onto 10 nm of Al_2O_3 on boron-doped Si(100). The typical pressure during evaporation is 7.5×10^{-7} Torr (1×10^{-4} Pa), and both materials are evaporated without exposure to air between the depositions. For Al_2O_3, the deposition rate is 2 Å/s, while the deposition rate for the Fe layer is 0.5 Å/s.

Following growth, carpet heights were obtained with a JEOL 6500 scanning electron microscope, and the nanotubes were imaged with a JEOL 2100 field emission gun transmission electron microscope. A typical scanning electron microscope image of a carpet sideview (a) and a close-up bundle-view (b) is shown in Figure 2. The image shown in Figure 2b emphasizes the alignment of nanotubes that is an inherent feature of the growth process of carpets. The heights reported throughout this

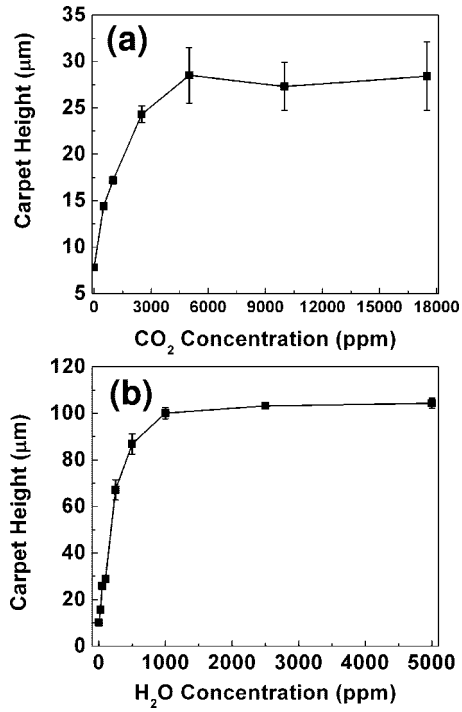

Figure 3. Dependence of the carpet height on the concentration of (a) CO_2 and (b) H_2O present in the reactor at 750 °C.

study are the averages of heights recorded every 5 mm along the length of the ~4 cm chip, along with error bars that are deemed appropriate for variation and measurement error. Raman spectra were obtained from a Kaiser Optical Systems Raman spectrometer with a fiber-optic probe, and fluorescence spectra were taken with an Applied NanoFluorescence Nanospectralyzer. The carpets were dispersed in 1 wt % sodium dodecylbenzylsulfonate (SDBS) after ultrasonication for 1 h.

Results and Discussion

The Role of an Oxidant during Growth. One of the primary objectives of this study is to develop an understanding of the role of the various oxidants that have previously been established as beneficial to SWNT growth, in the framework of the reactor described here. To do this, we study growth with various amounts of H_2O, CO_2, and O_2. The dependence of carpet height on the concentration of CO_2 and H_2O is shown in Figure 3. It should be noted that even trace amounts of O_2 present during the reaction is detrimental to the growth. When using a mixture of 1% O_2 in He, with as little as 1 sccm of this present during the growth period (0.01%, or 5 ppm O_2), absolutely no growth is observed. Even with as little as 0.1 sccm of 1% O_2 (0.001%), no growth is observed on the chip nearest to the hot filament, even though slight growth is observed toward the end side of the chip. This indicates that O_2 plays a severe detrimental role in the growth of carpets. However, upon inspection of Figure 3a, it is evident that the addition of a small concentration of CO_2 in the reaction gas mixture results in a significant enhancement of the carpet height. With an addition of only 500 ppm of CO_2, the carpet height increases from ~10 μm to ~15 μm. This continues until 5000 ppm, where the carpet height stays constant at ~27 μm with nearly 4 times the CO_2 concentration. Comparing this to Figure 3b, the presence of H_2O results in the same trend with respect to the carpet height, even though it is more pronounced. In fact, the saturation effect occurs at only ~1000 ppm of H_2O (instead of 5000 ppm), and the carpet height remains at ~105 μm tall with up to 5 times more water added to the reaction. This saturation effect of CO_2 and H_2O during carpet growth is an indication that a surface chemistry phenomenon is playing a significant role in the enhanced growth of carpets. As will be discussed later, in the case of water-assisted growth, it is likely the case that the water is reacting with the surface and forming surface-bound hydroxyl groups. This is likely to be the case on both the Al_2O_3 surface as well as on the edge of the Fe catalyst particles which are exposed to the underlying support. In the case of CO_2, water is most likely formed through a reaction with the H_2, namely,

$$H_{2(g)} + CO_{2(g)} \rightarrow CO_{(g)} + H_2O_{(g)} \quad (1)$$

which results in a reaction between the H_2O and the surface, leaving it hydroxylated, a feature that seems to be important for the growth process. This means that the enhanced carpet growth observed from the presence of CO_2 is most likely due to the same chemistry which drives the enhancement of carpet growth in the presence of only H_2. The difference is that it takes ~5 times more CO_2 to reach saturation due to the fact that CO_2 is a rather stable molecule, and surface hydroxylation is a reaction secondary to the formation of water. Also, it is interesting to note that the saturation of water and CO_2 result in different terminal heights of the carpets after 30 min of growth. This means that the rate-limiting step to achieving the best growth with CO_2 is the presence of a sufficient amount of H_2 for the reaction in eq 1 to take place.

In order to better understand the role of H_2O and CO_2, we perform experiments where the CO_2 or H_2O is present only for either the nucleation period (with the hot filament) or the growth period (after the filament is turned off), but not both. The results of these experiments are presented in Table 1. Here, the CO_2 and H_2O levels utilized are 4 sccm CO_2 and 100 sccm H_2/H_2O (~1 sccm H_2O)−both of which are in the "saturation" region where the growth is not further enhanced with additional oxidant presence. In the first case where the oxidant is only present during the nucleation period (in the first 30 s of growth when the hot filament is on), it is evident that the significant enhancement of growth observed with the oxidants present throughout the full growth period does not occur. In the particular case of H_2O-assisted growth, having this oxidant present during both nucleation and growth leads to ~10 times taller carpet than without any H_2O present. After turning off the H_2O 30 s into the growth, it is clear that the resulting carpet height (13.5 μm) is closer to the carpet height when no water is utilized (10.1 μm). On the other hand, beginning to bubble H_2 through H_2O directly following the hot filament exposure leads to a carpet with height of 107.1 μm, very close to the 103.3 μm observed when H_2O is on for both the nucleation and growth periods. This same general trend follows in the case

TABLE 1: Average Carpet Heights Measured for the Cases with and without an Oxidant (CO_2 and H_2O) Present during the Two Phases of Growth: (i) Reduction and Nucleation with Atomic Hydrogen Present (nucl + oxidant), and (ii) Post-Reduction Carpet Growth (growth + oxidant)[a]

nucl + oxidant?	growth + oxidant?	height, H_2O (μm)	height, CO_2 (μm)
N	N	10.1 ± 1	10.1 ± 1
Y	N	13.5 ± 1.5	18.27 ± 2
N	Y	107.1 ± 5	24.1 ± 3
Y	Y	103.3 ± 5	27.3 ± 3

[a] N = "No" and Y = "Yes." Approximate errors in height measurements are also included.

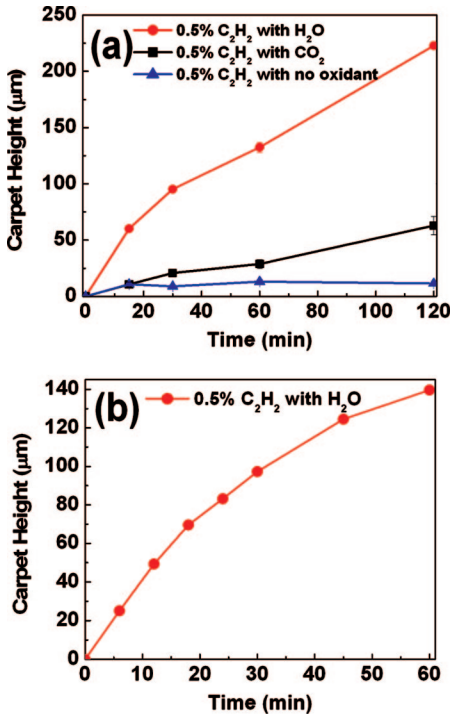

Figure 4. (a) Dependence of the carpet height on the growth time, for the three different cases of growth with CO_2, H_2O, and growth with no oxidant. (b) Dependence of the carpet height on the growth time with 2 sccm of H_2O present, during the early stages of growth compared to the plot shown in part (a).

of CO_2, even though it is not as enhanced since the terminal growth reported with CO_2 is only 2−3 times that with no oxidant at all. This emphasizes that the presence of an oxidant during growth results in a continuous reaction with the catalyst surface which is fundamentally important to achieving the enhancements to the carpet growth.

In terms of the growth enhancement observed with either CO_2 or H_2O present, it is important to consider whether this means that the growth rate has increased or the catalyst lifetime has been extended. Experiments were carried out to measure the carpet height as a function of growth time to study this effect, the results of which are presented in Figure 4a. In this case, H_2O and CO_2 were added into the reaction gas mixture at levels which resulted in the saturated carpet height as a function of oxidant concentration (Figure 3), which we perceive as being due to the saturation of the surface with hydroxyl groups. In the case of growth with no oxidant, the carpet height as a function of time is a straight line centered at about 10 μm. This indicates that, prior to 15 min of growth, the carpet growth has already been terminated. However, in the cases where CO_2 or H_2O are present, the carpet height clearly increases between the time intervals studied, emphasizing that the catalyst remains active at least up until 2 h of growth. Comparing the cases with 0.5% C_2H_2 with either CO_2 or H_2O, it is again evident that H_2O is more active at enhancing the growth rate, even though the presence of CO_2 does result in active catalyst up until 2 h. In addition, one may note that the three points between 30 min and 2 h seem to support the idea that growth is nearly linear over this time range, even though the points between 15 and 30 min seem to stray from the linear trend in all cases. This is further emphasized in Figure 4b, which shows the early stages of growth for a carpet with 0.5% C_2H_2 and 0.5% H_2O. It is clear from this plot that the early stages of growth develop through a nonlinear trend of carpet height with respect to growth

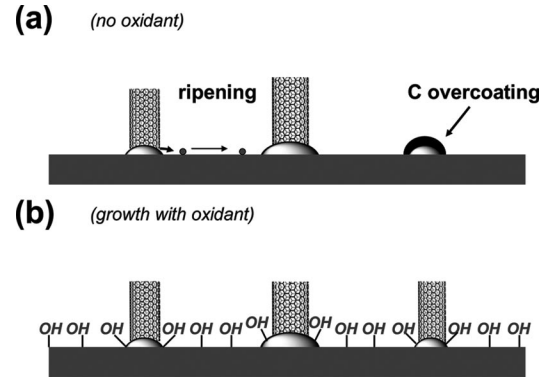

Figure 5. Schematic of effects which are occurring on the catalyst during growth (a) without, and (b) with an oxidant present. In the top panel, carbon overcoating and Ostwald ripening[35] are labeled as potential termination mechanisms, where in the bottom panel, the hydroxyl-terminated surface protects against such effects.

time. As the carpet is a relatively dense material, it is expected that this signifies a transition between two different growth modes of a carpet. The first of these is where the catalyst is freely exposed to the incoming C_2H_2, and the growth rate is limited only by the C_2H_2 flux.[28] The second case is when a substantial amount of carpet has already been catalyzed; the carbon feedstock supplied to the catalyst is through diffusive flux to the catalyst after collisions with the nanotubes in the carpet. As we observe, after approximately 30 min, the growth is solely due to diffusive flux of carbon resulting in a constant rate of carbon being supplied to the catalyst surface.

As a result of our experiments, we are able to construct a picture that follows our interpretation of the effect of H_2O and CO_2 in the framework of our experimental observations, shown in Figure 5. In the first case, where no oxidant is present, the carpet growth terminates after a relatively short exposure to carbon. Although the concept of why termination occurs is still being heavily researched and is likely to be a complicated phenomenon, there are two primary reasons why this occurs. The first of these is based on the fact that H_2O and CO_2 both will act to etch away amorphous carbon that forms in the first stages of growth and throughout the growth process. Since there is a broad catalyst size distribution (and hence, a broad nanotube diameter distribution, which will be discussed at a later point), a constant flux of carbon to the surface will result in some nanotubes growing faster than others. This variation in growth rate will be ultimately limited by the uniform growth rate of the carpet, and will result in many of the particles beginning to become too saturated with carbon and forming a carbon shell (and a carbide).[33,34] As a result, this will create a uniform drag force on the growing carpet, which will further this effect until collective growth termination occurs. The second effect which is illustrated in the top panel of Figure 5 is Ostwald ripening of the catalyst particles over time. Utilizing state-of-the-art imaging techniques, we have recently established this effect as being a serious issue in carpet growth[35] and proved that, without an oxidant present during growth, only 5 min of annealing in H_2 under growth conditions leads to ripening into large (>8 nm) particles which will no longer be conducive to SWNT carpet growth. Thus, carpet growth without an oxidant present is plagued with two potential termination mechanisms which occur relatively quickly during the growth period, making this form of growth short and inefficient.

On the other hand, the bottom panel of Figure 5 illustrates the effect of having an oxidant present on the catalyst surface during growth. Whereas the CO_2 and H_2O are surely acting to

etch away excessive carbon to extend the catalyst lifetime, we suggest that they are also acting to hydroxylate the surface and make it less likely for ripening to take place. An argument for surface hydroxylation is straightforward, based upon the results from data presented thus far, emphasizing that the addition of H_2O is initializing surface chemistry with the catalyst and support which is dramatically enhancing the catalyst lifetime. Furthermore, recent studies identifying Ostwald ripening as being an issue in this growth process[35] also emphasize that the addition of a small amount of water during growth slows the ripening rate substantially, allowing for longer catalyst lifetimes due to better catalyst stability. Therefore, having a hydroxylated surface will result in the "pinning" of any mobile Fe atoms near the edge of the catalyst to surface-bound oxygen groups which will stabilize them. In light of this, it should be noted that previous studies using gas-phase SWNT growth techniques have emphasized the role of H_2O and CO_2 in the process of etching away excess C,[22,23] even though these studies are not conducted on a surface where such ripening effects may *also* tend to inhibit growth. As a result, surface hydroxylation and amorphous carbon etching are two major roles of an oxidant on this carpet growth process, and these are necessary in any similar carpet growth process as well.

In the spirit of understanding the effects of H_2O and/or CO_2 on the properties of the nanotubes themselves, detailed analysis of the effect of H_2O and CO_2 concentration on Raman D and G band ratios and photoluminescence (PL) intensities was performed. In both cases, the D:G ratio was found to be invariant with increasing concentration of oxidant (within 10%), and no difference was observed in the absorbance-normalized PL measurements as the oxidant concentration increased—indicating that the relative ratios of small-diameter nanotubes are approximately the same in each case. In addition, Raman measurements were performed by focusing the laser spot on the side of the carpet (with the exception of the very top of the carpet). In these experiments, no change in D:G ratio could be observed between the top side of the carpet and the bottom with spectra taken at nine uniformly spaced spots along the carpet height. These results indicate a few important aspects of growth with an oxidant present: (i) the oxidant does not seem to improve the inherent "quality" of the nanotubes, (ii) the oxidant does not seem to fundamentally change the distribution of nanotube diameters present in the carpets, and (iii) growth with the oxidant results in a carpet that is highly uniform from top to bottom in terms of D:G ratio and RBMs. These points are important to make, as they precede our investigation on the effect of temperature, where we *do* find differences between the nanotubes with Raman scattering and PL measurements.

The Role of Reactor Temperature during Growth. One of the most important and fundamental parameters in any growth study is the temperature at which the reaction is observed to take place, and how this temperature affects the properties of the resulting material that is grown. Previous modeling and experiments establish that the growth of carpets is a process highly sensitive to temperature. In the framework of the modeling technique conceived by Wood et al.,[28] the temperature defines the rate at which the carbon is transferred from the surface of catalyst particle to the growing nanotube, which ultimately defines the growth rate of the nanotube and the number of walls each nanotube contains. At the highest temperatures where growth can be achieved, only SWNT growth is observed due to the increased rate at which carbon is being transported through the catalyst particle and deposited onto the growing nanotube. However, at the lowest temperatures where nanotube growth takes place, this modeling approach emphasizes that the diffusion rate of the catalyst particle is lower, meaning that the rate at which carbon is arriving at the surface of the particle is greater than the rate at which the carbon can be incorporated into a single wall, resulting in the emergence of a second or third wall to the growing nanotube. As we will describe in detail here, the general nature of our results seem to be in excellent agreement with the predictions of this modeling approach.

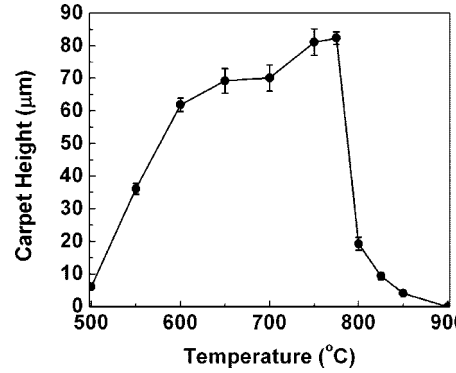

Figure 6. Carpet height as a function of temperature, for temperatures that range between 500 and 900 °C in carpet growth with 2 sccm of H_2O present.

In all measurements studying the role of temperature upon carpet growth, we utilize a concentration of H_2O in the reaction gas mixture that is found to be well beyond the point at which we expect hydroxyl saturation to occur (2 sccm H_2O). In order to study the effect of temperature upon carpet growth, we compare the height of carpets grown at several different temperatures, which is presented in Figure 6. We find that, below a temperature of 500 °C, no carpet growth is observable, even though the surface of the growth substrate is blackened by a thin sheet of nanotubes during growths at 450 °C. However, at 500 °C and above, the carpet height increases with temperature up until a critical temperature is reached at 775 °C, where a further increase in temperature leads to a sudden drop-off in carpet height. This sort of behavior has been reported in the past,[27] and is defined as the effect of catalyst "poisoning." Although we are still in the process of a detailed study of the cause of this effect, it is likely that one or a combination of (i) Fe-carbide formation, (ii) Ostwald ripening, or (iii) FeO intercalation to the Al_2O_3 support, are responsible for this.

In order to understand the effect that temperature has upon the properties of the nanotubes that are grown, we dispersed the carpet-grown nanotubes in 1 wt % sodium dodecylbenzylsulfonate (SDBS) via bath sonication for 1 h. Although an effort was made to achieve optical densities that were similar by eye, visible absorbance measurements were also taken to normalize the intensities of the photoluminescence (PL) measurements to the concentration of the dispersed SWNT solution. The concentrations were calculated based upon a previously established laboratory standard by measurement of absorbance at 763 nm. The resulting normalized PL data for excitations at 660 nm (utilized for carpet growth) at different temperatures is presented in Figure 7. It should be noted that data for temperatures below 600 °C is not shown in Figure 7 due to the lack of any PL signal above background noise. Even at 600 °C, the PL signal is at least an order of magnitude smaller than at a slightly higher temperature of 650 °C. This emphasizes that there is some fundamental difference between growth at 600 and 650 °C, even though the carpet height measurements indicate that carpets grow at both temperatures. Interestingly, as the temperature is

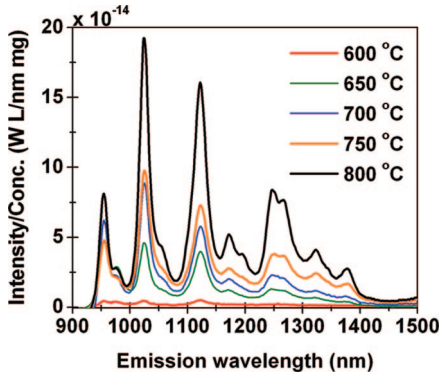

Figure 7. Photoluminescence spectra from 660 nm excitations of SDBS dispersed carpet nanotubes grown at different temperatures. Absolute intensities for a fixed amount of time are reported normalized to the concentration of each individual solution.

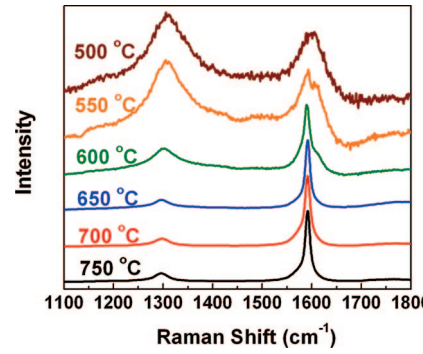

Figure 8. D and G bands from liquid-phase Raman spectra utilizing 785 nm excitations through a fiber-optic probe. Spectra are normalized to the G band in all cases.

further increased, the normalized PL intensity also increases, indicating a more significant presence of smaller-diameter SWNTs. It should be noted at this point that the PL measurements can only sample a small window of the large range of nanotube diameters that are present in carpets.[36,37] Therefore, one cannot infer that changes in the observed peaks in the PL spectra are indicative of differences in the distribution of nanotube diameters present in carpets. However, based on extensive studies which have proven that a double-walled or multiwalled nanotube (DWNT or MWNT) will not fluoresce,[38] the observation of PL and the absolute intensity of that PL signal can be utilized as an indication of the presence of small-diameter SWNTs in our carpets. A consistent trend in Figure 7 is that carpet growth at the highest possible temperature yields the greatest normalized PL intensity—suggesting the greatest amount of small diameter SWNTs. This also holds true for growth at 800 °C, which is on the edge of the "poisoning" regime, directly above the temperature point in Figure 6 where the greatest carpet height is observed. The normalized PL intensity for a carpet grown at 800 °C is the greatest, indicating that the higher temperatures yield the best small-diameter SWNT growth—a concept consistent with the modeling approach by Wood et al.[28]

In addition to PL measurements, we also observe a similar effect by analyzing the temperature dependence of 785 nm Raman spectra presented in Figure 8. The data presented in Figure 8 have been corrected for the baseline noise and normalized to the G-peak for each temperature. As is evident from Figure 8, a large D peak is a signature of carpet growth at the lowest temperatures. Since absolutely no PL intensity is observed from dispersed nanotubes from either of these carpets (500 and 550 °C), it is evident that there is no trace of any small-diameter SWNTs present in these. Therefore, this large D-band can be attributed to the formation of an additional wall or walls to the nanotubes.[27] This observation of a larger D band is regarded as the signature of a significant number of sp^3 defects forming in multiwalled nanotubes grown at low temperatures. In the concept of the model that we have adopted so far, this is consistent because if the rate of growth of the nanotube is limited by the outermost SWNT that is growing, it is likely that additional walls will be defective due to the fact that there is a very small probability the incoming carbon flux exactly matches the amount of carbon needed to achieve perfect graphitization in the inner wall(s) and keep up with the growth rate of the outer wall. Analagous to the PL spectra shown in Figure 7, we also observe in Raman spectra that there is a well-defined transition between the D and G peaks for nanotubes grown at 600 °C, and the D and G peaks for those grown at 650 °C. Although the D peak is lower for the nanotubes grown at 600 °C than for those grown at lower temperatures, there is a significant difference between the D peak for the nanotubes grown at 600 °C and those grown at higher temperatures (650−750 °C). Also, the nanotubes grown between 500−600 °C have a higher-frequency shoulder in the G-band than what is observed for high-quality SWNT material. This shoulder is centered at a frequency close to 1615 cm^{-1}, and corresponds to a D′ peak that is typically observed for multiwalled carbon nanotubes that tend to be defective.[39] It is likely that the bath sonication process for dispersing the nanotubes contributed to the formation of this D′ peak, as previous studies on cut MWNT also observed the emergence of a D′ peak after only 10 min of mild cutting.[40] However, between the temperatures of 650−750 °C, there is little change in the D band intensity, and the G band can be described as a single Lorentzian centered about ∼1592 cm^{-1} (no high frequency shoulder). This emphasizes that the temperature dependence observed in PL measurements and Raman spectra emphasizes a transition between a state where the nanotubes are composed of greater than one wall (and highly defective) to a state where they have only a single wall (and are of high quality).

In order to verify the picture already established through PL and Raman spectra, we performed high resolution transmission electron microscopy (HR-TEM) on nanotubes grown from carpets at (i) 600 °C, where the transition between MWNT and SWNT is observed, and (ii) 775 °C, where the greatest population of SWNTs is expected based on Raman and PL spectra. Representative TEM images of both cases are shown in Figure 9. In the case of carpets grown at 775 °C (Figure 9a), we observe very few nanotubes in the TEM measurements that have greater than one wall. The majority of nanotubes are SWNTs, but the diameter distribution is broad. From our observations, the SWNTs have diameters ranging between 0.8 and 4 nm, which is consistent with the general diameters of nanotubes presented in growth methods such as water-assisted supergrowth of Hata et al.[13] However, upon decreasing the temperature to 600 °C (Figure 9b), we observe that nearly all of the nanotubes are now DWNTs, with only a few exceptions of SWNTs (less than 10%), and some defective material. This verifies that the reason for both the lack of PL intensity and the enhanced D band between the growths at 775 and 600 °C is that the nanotubes are sprouting an additional wall in the carpet grown at 600 °C, resulting in a slightly higher D band, and no PL intensity. A further decrease in the growth temperature results in an increased D band, emphasizing that the nanotubes present in the carpets are now MWNT.

This emphasizes that temperature does play a significant role in the quality and type of nanotubes grown in carpets in the

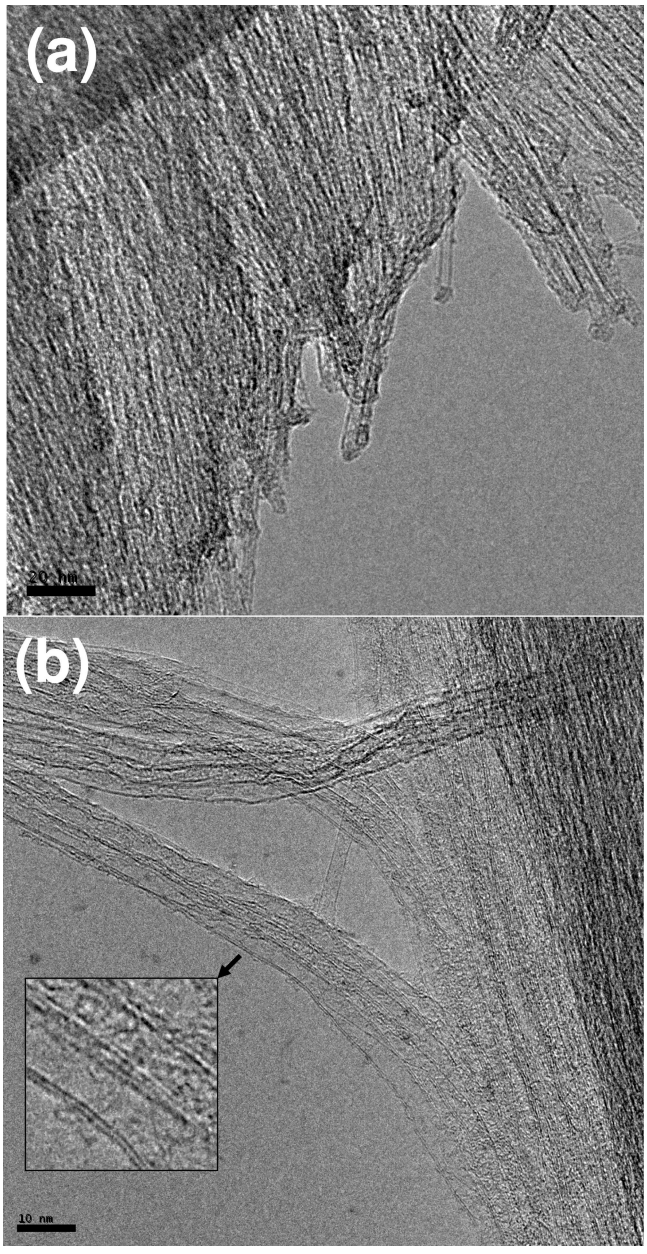

Figure 9. Transmission electron microscope (TEM) images of nanotubes grown from carpets at (a) 775 °C, and (b) 600 °C. Images from 600 °C indicate that the nanotubes are primarily DWNTs, with only one visible SWNT in the image. Length scale bar is (a) 20 nm and (b) 10 nm. Inset in (b) shows a close-up view of the DWNT on the edge of the bundle.

CVD process. Although our emphasis is on the production of high-quality SWNTs, we also find that simply changing the growth temperature can result in controllable growth of DWNTs, or even the growth of few-walled nanotubes at lower temperatures. This is an important point to make, as it often is attractive for some applications to have strictly DWNTs or few-walled nanotubes in the sample, as opposed to just SWNTs. However, in addition to control of the nanotubes that can be grown in this method, it is also of interest to produce large quantities of the specified material. In the next section, we will discuss experiments focused on producing ultralong carpets by only increasing the carbon collision rate with the catalyst surface.

The Role of Reaction Gas Pressure during Carpet Growth. As we have described previously, the reactor utilized for this study operates at low pressures (1.4 Torr) due to the continuous pumping of the reaction gas mixture through a scroll pump. The pressure in the reaction chamber is measured directly downstream from the reactor by a capacitance monometer and is equivalent to a measurement of the reaction gas flow velocity as long as the amount of gas that is continuously supplied to the reactor is known. In this sense, having the lowest possible pressure in the chamber results in having the largest reaction gas flow velocity, which will minimize the number of collisions (or carbon flux) between gas molecules in the reaction mixture and the catalyst surface. As the pressure is increased, the flow velocity will decrease allowing for more collisions between carbon feedstock molecules (C_2H_2) and the catalyst surface, and hence, the chemical potential will drive the reaction to occur at a greater rate. This is important for growth with C_2H_2, since previous studies have shown that it is over an order of magnitude more reactive than any other growth gas (CH_2, C_2H_4, etc.) in decomposition over Fe catalyst.[18] As a result, the ability to control the carbon flux to the catalyst surface by operating at the lowest pressure allows for the widest temperature range in which SWNT growth can be achieved, even though the yield of nanotubes relative to incoming carbon is low since only a small percentage of the available carbon is actually catalyzed into nanotubes. In order to increase the yield, one can simply increase the pressure of the reaction gas inside of the quartz tube where the carpet is growing. We achieve this by partially closing a manual valve located directly before the scroll pump, decreasing the flow velocity of the gas until the pressure stabilizes at desired value. Once this pressure stabilizes, we rapidly insert the growth substrate into the reactor heated to 750 °C and expose the substrate to atomic hydrogen for the typical 30 s. It should be noted that the carpet growth occurs uniformly over the length of the chip until ~35 Torr, where the carpet height on the side nearest to the hot filament is up to 35% different than the carpet height on the side furthest from the hot filament. This is expected to be an effect of uneven atomic hydrogen exposure due to a shorter, finite diffusion distance of atomic hydrogen at an elevated pressure. Therefore, we only measure the average carpet height for carpets grown between 1.4 and 35 Torr, the results of which are presented in Figure 10a. In this plot, it is evident that the curve is not a straight line, as one would expect if the carpet height scales linearly with the number of collisions between C_2H_2 molecules and the catalyst surface. This is most likely an effect that is due to the requirement that an active carbon source must penetrate the carpet and diffuse through the network before it can reach the catalyst particles at the base of the substrate. This sort of effect due to diffusion-related carbon supply has been observed elsewhere in situ during the growth of long carpets.[41] In our experiments, we find that one can increase the pressure in the quartz tube from 1.4 to 25 Torr, which results in a carpet that grows to nearly 600 μm in the course of only 30 min. This emphasizes the same sort of high-yield growth that is achieved during supergrowth utilizing ethylene.[13] However, one may notice that an increase of ~18 in pressure only corresponds to a carpet that is about 6 times taller. This indicates that either diffusion limitations on the growth rate are affecting the amount of carbon that makes it to the catalyst at the base of the carpet, or else there is an abundance of nanotubes which have now sprouted additional walls. We note that only near a temperature close to where poisoning occurs can we grow such a long carpet by increasing the carbon flux. Growth at lower temperatures (600 °C) results in early termination of the catalyst, probably due to the overwhelming amount of carbon that is being introduced to a catalyst particle that can not support such a rapid

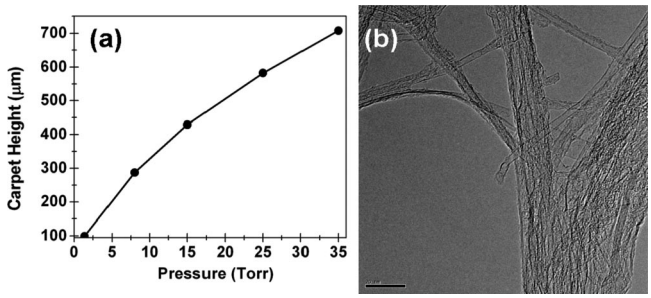

Figure 10. (a) Plot of carpet height as a function of pressure for experiments where the temperature is fixed at 750 °C, but the carbon flux is increased by decreasing the flow velocity of reaction gas. (b) Transmission electron microscope (TEM) image of typical material obtained in growth at 25 Torr, suggesting the presence of a mixture few-walled nanotubes, SWNTs, and some large structures resembling SWNTs. Scale bar in (b) is 20 nm.

rate of growth. In order to better understand this effect, we imaged carpets grown at 25 Torr at 750 °C under TEM, with a representative TEM image presented in Figure 10b. Although we do see a significant (majority) population of SWNTs, we also observe the presence of few-walled nanotubes (2−5 walls), among a population of very large-diameter SWNTs. One such large-diameter SWNT is shown in the central region of Figure 10b, and corresponds to a SWNT with a diameter of ∼12 nm. Raman spectra of carpets grown at 25 Torr indicate an enhanced D band intensity (G/D ≈ 1.8), which is typically due to a reasonable population of few-walled nanotubes, as discussed previously. However, TEM images confirm that between 50−75% of the nanotubes have only a single wall, emphasizing this material is a SWNT/FWNT mixture. In terms of optimizing growth with respect to total carpet height, it may be acceptable to have a reasonable FWNT population (two to four walls) mixed with SWNTs for some applications where the ultrahigh aspect ratio of the long nanotubes is sought. However, in principle, if one is able to achieve a significant level of control on the catalyst size, and carry out the reaction at a temperature close to the poisoning temperature, it is reasonable that such a long carpet can be purely composed of high-quality SWNTs. This would be the most efficient way to produce SWNTs in this method, even though it may take a reasonable level of catalyst engineering to maintain a well-defined catalyst size. Although we are underway in achieving this by synthesizing Fe_3O_4 particles capped in an organic ligand, we took the next step to investigate if this substantial growth rate that is maintained at 25 Torr can be sustained for longer than 30 min. After growth for a period of 6 h, we observe that we obtain a carpet that is between 3 and 3.5 μm−a length that would be expected if growth was continuous over this interval of time. A photograph of this long carpet, grown for 6 h at 25 Torr, is shown in Figure 11. The overall length of the carpet is found to be between 3−3.5 mm, with the carpet edges taller due to the fact that diffusion limitations are not introduced at the edge of the carpet in the same way that they are in the center. Weighing this chip before and after growth, the ∼1 cm by 1 cm chip grew 9.6 mg of nanotubes in total after 6 h. Although this yield is still low compared to the typical yields from methods such as HIPCO, a scale-up process could potentially produce grams of nanotubes per day in this method. In addition, since the catalyst remains fixed at the base of the carpet, the nanotubes are ultralong and free of Fe impurities, leaving the purification process straightforward. The only issue that plagues this growth method is the less-than-optimal nanotube length that will always be achieved due to the fact that the carpet grown

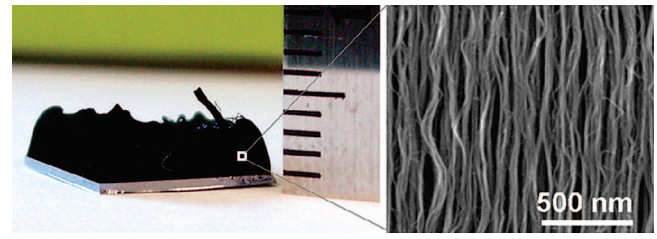

Figure 11. Photograph of a 3−3.5 mm long carpet obtained after growth for 6 h at 25 Torr of pressure. A high magnification SEM image depicts the bundle structure of nanotubes in the carpet.

inside from the edge of the chip is going to suffer from serious limitations due to uneven rates of carbon flux to the catalyst based on diffusion limitations. This opens the door for new and innovative techniques to grow aligned nanotubes where the catalyst will always be exposed to the carbon source, and aligned nanotube growth can potentially take place over meters and meters of distance. Inasmuch as the process of carpet growth with a fixed catalyst layer at the base can be optimized on a small scale, as we show here, future demands for the ultralong nanotubes that are achieved in this method will require optimization of the process itself in order to achieve the goals that still linger from the thought-inspiring concepts that have been conceived in the past few decades, such as the carbon nanotube space elevator.[42]

Conclusions

We demonstrate here the ability to optimize the process of growing vertically aligned single-walled carbon nanotubes in three subsequent steps. First of all, we optimize the growth of carpets by including the presence of an oxidant in the reaction gas mixture. We find that water provides a highly efficient route toward catalyst preservation by surface hydroxylation as well as the etching of amorphous carbon during the growth process. This results in active catalyst sites for highly extended growth duration, and protects the catalyst from ripening and/or carbide formation, two potential effects responsible for the early termination of growth without the presence of an oxidant. Next, we provide a detailed study of the effect of temperature on the nanotubes grown in the carpet, observing that temperature allows for the ability to tune the deposition rate of carbon on the growing nanotube, leading to controllable growth that can be varied between high-quality SWNT growth and more defective MWNT carpets based on whether the carbon flux to the surface overwhelms the rate at which a SWNT can grow. We find that high-quality SWNT growth is always obtained closest to the "poisoning" temperature and MWNT growth is obtained during growth at the lowest temperatures where carpets are found to grow. Finally, we emphasize that by increasing the carbon collision rate at a temperature that is near where poisoning occurs, we can achieve the growth of ultralong carbon nanotubes in a highly efficient way. We find that a 6 h growth can yield a carpet that is between 3−3.5 mm long. This work emphasizes that optimization of carpet growth can be achieved in a systematic way, and that carpet growth in a hot filament CVD apparatus is geared toward this type of optimization.

Acknowledgment. We thank D. Natelson's group for use of evaporation equipment vital to the completion of this study. We also thank N. Nicholas, E. Haroz, N. Alvarez, H.K. Schmidt, C. Kittrell, and J. Tour for discussions. This work was partially supported by the Air Force Office of Scientific Research.

References and Notes

(1) Bethune, D. S.; Klang, C. H.; Devries, M. S.; Gorman, G.; Savoy, R.; Vazquez, J.; Beyers, R. *Nature* **1993**, *363*, 605.

(2) Murakami, Y.; Chiashi, S.; Miyauchi, Y.; Minghui, H.; Ogura, M.; Okubo, T.; Maruyama, S. *Chem. Phys. Lett.* **2004**, *385*, 298.

(3) Fan, S. S.; Chapline, M.; Franklin, N. R.; Tombler, T. W.; Cassell, A. M.; Dai, H. *Science* **1999**, *283*, 512.

(4) Dalton, A. B.; Collins, S.; Razal, J.; Munoz, E.; Ebron, V. H.; Kim, B. G.; Coleman, J. N.; Ferraris, J. P.; Baughman, R. H. *J. Mater. Chem.* **2004**, *14*, 1.

(5) Futaba, D. N.; Hata, K.; Yamada, T.; Hiraoka, T.; Hayamizu, Y.; Kakudate, Y.; Tanaike, O.; Hatori, H.; Yumura, M.; Iijima, S. *Nat. Mater.* **2006**, *5*, 987.

(6) Wood, J. R.; Wagner, H. D. *Appl. Phys. Lett.* **2000**, *76*, 2883.

(7) Kong, J.; Franklin, N. R.; Zhou, C. W.; Chapline, M. G.; Peng, S.; Cho, K. J.; Dai, H. *Science* **2000**, *287*, 622.

(8) Ge, L.; Sethi, S.; Ci, L.; Ajayan, P. M.; Dhinojwala, A. *Proc. Natl. Acad. Sci. U.S.A.* **2007**, *104*, 10792.

(9) Sethi, S.; Ge, L.; Ci, L.; Ajayan, P. M.; Dhinojwala, A. *Nano Lett.* **2008**, *8*, 822.

(10) Majumder, M.; Chopra, N.; Andrews, R.; Hinds, B. J. *Nature* **2005**, *438*, 44.

(11) Corry, B. *J. Phys. Chem. B* **2008**, *112*, 1427.

(12) Pint, C. L.; Pheasant, S. T.; Pasquali, M.; Coulter, K. E.; Schmidt, H. K.; Hauge, R. H. *Nano Lett.* **2008**, *8*, 1879.

(13) Hata, K.; Futaba, D. N.; Mizuno, K.; Namai, Y.; Yumura, M.; Iijima, S. *Science* **2004**, *306*, 1362.

(14) Futaba, D. N.; Hata, K.; Yamada, T.; Mizuno, K.; Yumura, M.; Iijima, S. *Phys. Rev. Lett.* **2005**, *95*, 056104.

(15) Noda, S.; Hasegawa, K.; Sugime, H.; Kakehi, K.; Zhang, Z.; Maruyama, S.; Yamaguchi, Y. *Jpn. J. Appl. Phys.* **2007**, *46*, L399.

(16) Chakrabarti, S.; Nagasaka, T.; Yoshikawa, Y.; Pan, L.; Nakayama, Y. *Jpn. J. Appl. Phys.* **2006**, *45*, L720.

(17) Pint, C.; Pheasant, S.; Nicholas, N.; Horton, C.; Hauge, R. *J. Nanosci. Nanotechnol.* **2008**, *8*, 6158.

(18) Eres, G.; Kinkhabwala, A. A.; Cui, H.; Geohegan, D. B.; Puretzky, A. A.; Lowndes, D. H. *J. Phys. Chem. B* **2005**, *109*, 16684.

(19) Zhang, G.; Mann, D.; Zhang, L.; Javey, A.; Li, Y.; Yenilmez, E.; Wang, Q.; McVittie, J. P.; Nishi, Y.; Gibbons, J.; Dai, H. *Proc. Natl. Acad. Sci. U.S.A.* **2005**, *102*, 16141.

(20) Wen, Q.; Qian, W.; Wei, F.; Ning, G. *Nanotechnology* **2007**, *18*, 215610.

(21) Zhang, C.-M.; Fu, Y.-b.; Chen, Q.; Zhang, Y.-F. *Front. Mater. Sci. China* **2008**, *2*, 37.

(22) Nasibulin, A. G.; Brown, D. P.; Queipo, P.; Gonzalez, D.; Jiang, H.; Kauppinen, E. I. *Chem. Phys. Lett.* **2006**, *417*, 179.

(23) Nasibulin, A. G.; Queipo, P.; Shandakov, S. D.; Brown, D. P.; Jiang, H.; Pikhitsa, P. V.; Tolochko, O. V.; Kauppinen, E. I. *J. Nanosci. Nanotechnol.* **2006**, *6*, 1233.

(24) Eres, G.; Puretzky, A. A.; Geohegan, D. B.; Cui, H. *Appl. Phys. Lett.* **2004**, *84*, 1759.

(25) Zhong, G. F.; Iwasaki, T.; Honda, K.; Furukawa, Y.; Ohdomari, I.; Kawarada, H. *Chem. Vap. Deposition* **2005**, *11*, 127.

(26) Zhong, G. F.; Iwasaki, T.; Robertson, J.; Kawarada, H. *J. Phys. Chem. B* **2007**, *111*, 1907.

(27) Puretzky, A. A.; Geohegan, D. B.; Jesse, S.; Ivanov, I. N.; Eres, G. *Appl. Phys. A* **2005**, *81*, 223.

(28) Wood, R. F.; Pannala, S.; Wells, J. C.; Puretzky, A. A.; Geohegan, D. B. *Phys. Rev. B* **2007**, *75*, 235446.

(29) Xu, Y.-Q.; Flor, E.; Schmidt, H.; Smalley, R. E.; Hauge, R. H. *Appl. Phys. Lett.* **2006**, *89*, 123116.

(30) Xu, Y.-Q.; Flor, E.; Kim, M.; Hamadani, B.; Schmidt, H.; Smalley, R. E.; Hauge, R. H. *J. Am. Chem. Soc.* **2006**, *128*, 6560.

(31) Pheasant, S. T. Ph.D. Dissertation under R.E. Smalley and R.H. Hauge, 2007, Rice University.

(32) Larjo, J.; Koivikka, H.; Li, D.; Hernberg, R. *Appl. Opt.* **2001**, *40*, 765.

(33) Bower, C.; Zhou, O.; Zhu, W.; Werder, D. J.; Jim, S. *Appl. Phys. Lett.* **2000**, *77*, 2767.

(34) Harutyunyan, A. R.; Awasthi, N.; Jiang, A.; Setyawan, W.; Mora, E.; Tokune, T.; Bolton, K.; Curtarolo, S. *Phys. Rev. Lett.* **2008**, *100*, 195502.

(35) Amama, P. B.; Pint, C. L.; McJilton, L.; Kim, S. M.; Stach, E. A.; Murray, P. T.; Hauge, R.; Maruyama, B. *Nano Lett.* **2009**, *9*, 44–49.

(36) Bachilo, S. M.; Strano, M. S.; Kittrell, C.; Hauge, R. H.; Smalley, R. E.; Weisman, R. B. *Science* **2002**, *298*, 2361.

(37) Okazaki, T.; Saito, T.; Matsuura, K.; Ohshima, S.; Yumura, M.; Oyana, Y.; Saito, R.; Iijima, S. *Chem. Phys. Lett.* **2006**, *420*, 286.

(38) Tsyboulski, D. A. and Weisman, R. B. Unpublished.

(39) Jorio, A.; Pimenta, M. A.; Souza Filho, A. G.; Saito, R.; Dresselhaus, G.; Dresselhaus, M. S. *New J. Phys.* **2003**, *5*, 139.

(40) Park, K. C.; Fujishige, M.; Takeuchi, K.; Arai, S.; Morimoto, S.; Endo, M. *J. Phys. Chem. Solids* **2008**, *69*, 2481.

(41) Puretzky, A. A.; Eres, G.; Rouleau, C. M.; Ivanov, I. N.; Geohegan, D. B. *Nanotechnology* **2008**, *19*, 055605.

(42) Yakobson, B. I.; Smalley, R. E. *Am. Sci.* **1997**, *85*, 324.

JP8070585